

Article

Improve Design Antenna by Using Machine Learning and Material

Azhaar A. Shalal¹, Hazeem B. Taher², Mahmood F. Mosleh³, Azhaar A. Hussan^{*4}

1. Department of Computer engineering College of Engineering , shatrah university, shatrah , Iraq
 2. Ministry of Higher Education/Department of Scholarships and Relations
 3. Department of Computer Engineering Techniques, Electrical Engineering Technical College, Middle Technical University, Baghdad, Iraq
 4. Department of computer science Computer science and mathematics College, Kufa university, Kufa, Iraq
- * Correspondence: azhaara.alkhafaji@student.uokufa.edu.iq

Abstract: This study presents improve a MIMO antenna system using machine learning, aiming for broad frequency coverage, high gain, compact size, and excellent isolation. The antenna employs four elements arranged orthogonally on a compact substrate, integrating a multi-slotted radiating patch and a partial ground plane. The absence of a meta surface is compensated by leveraging machine learning techniques to optimize the antenna's performance. Through regression methods, particularly linear regression, the antenna achieves remarkable accuracy in gain and efficiency validation. This approach underscores the crucial role of machine learning in refining antenna designs, enhancing their effectiveness in various applications such as Vehicle-to-Everything (V2X) communications within the 5G application.

Keywords: Index Terms - Antenna, CST, MIMO, Machine learning, 5G

Citation: Shalal, A. A., Taher. H. B., Mosleh, M. F., Hussan, A. A. Improve Design Antenna by Using Machine Learning and Material. Central Asian Journal of Mathematical Theory and Computer Sciences 2025, 6(2), 235-247.

Received: 12th Mar 2025
Revised: 17th Mar 2025
Accepted: 20th Mar 2025
Published: 26th Mar 2025



Copyright: © 2025 by the authors. Submitted for open access publication under the terms and conditions of the Creative Commons Attribution (CC BY) license (<https://creativecommons.org/licenses/by/4.0/>)

1. Introduction

Innovative antenna designs have emerged in response to the surge in demand for fast data transmission and connectivity in (IoT) applications and the rapid growth of wireless communication technologies. As wireless communication technology has evolved from 1G to 5G networks, significant strides have been made in the sector. The ideal operation of Internet of Things (IoT) systems requires the improvement of reliability, the reduction of power consumption, and the growth of channel capacity [1]. The capacity to provide higher data rates and improved connectivity make super wideband (SWB) technology the most sought-after alternative in modern wireless communication [2].

As the way for Ultra-wideband (UWB) technology, the frequency range of 3.1-10.6 GHz has been reserved for wireless applications by the Federal Communications Commission (FCC). While UWB is concerned with a certain frequency range, SWB is more generalized. Multipath fading is the culprit responsible for the downfall of wide-band antenna systems. Multiple input multiple output (MIMO) technology can be used to mitigate multipath fading issues, as shown in References [3], [4]. (MIMO) technology uses a constrained array of antenna elements to reduce the effects of multipath fading via mutual coupling and interference [5]. Using a number of antennas at the sending and receiving ends, a wireless communication method known as Multiple-Input Multiple-Output (MIMO) is employed.

The limited isolation between difference antenna elements, known as confusion or mutual coupling, is an extra challenge when developing Multiple-Input Multiple-Output (MIMO) systems. The system's overall performance could be negatively impacted by this reciprocal coupling. Parasitic decoupling structures, flawed ground systems, slotted stubs, metamaterials, and meta-surfaces were among the methods used by researchers to overcome this obstacle and increase the obtained gain [6], [7], [8], [9].

The use of metamaterials in antenna systems is multifaceted [10], [11]. For instance, to alter the radiation pattern in the intended direction, enhance the bandwidth, and realize more gain while decreasing efficiency. In [12], the authors improve the antenna's bandwidth by using a metamaterial transmission line. In a separate study, the author increased the impedance bandwidth by employing a T-matching network that was inspired by metamaterials [13]. When configuring MIMO, isolation is a crucial component. Antenna element isolation was improved by numerous researchers through the use of metamaterials and meta-surfaces [14]. When used to periodic metamaterial-photonic bandgap, isolation increase can be achieved [15].

In a multiple-input multiple-output (MIMO) setup, some researchers have employed metamaterial electromagnetic bandgap to improve isolation between nearby antenna elements [16], [17]. Some of the decoupling structures investigated in [18] include modified U-shaped resonators, which can improve isolation. Another study found that by inserting a peripheral slot, the authors were able to decrease the mutual coupling [19].

Several of the antennas employed in the aforementioned investigations failed to adequately address the issues raised in the cited works [20], [21], [22], [23], [24], [25], [26], [27], [28], [29], [30], [31], [32], [33], [34], [35], [36], [37], [38]. Prior to the proposed design, the majority of works were either very little or very large, but they lacked proper isolation, efficiency, or gain. Making it possible for the Internet of Things and lightning-fast wireless Internet A small multiple-input multiple-output antenna that excels in efficiency, gain, and minimal coupling is required.

A Super-Wideband MIMO Antenna is described in [2] using a grounded stub. Its isolation is 20 dB, although it has low gain and is rather large for Internet of Things applications. Figure 7 shows a 20 dB isolation ultra-wideband antenna that is optically transparent. The main issues with this antenna are its low gain and inefficiency. Their efficiency is 60% and the gain is 2.5 dB. Several research have used parasitic decoupling structures on antennas to improve isolation and gain [8], [25], [26]. In order to attain high gain and strong isolation (6.94 dBi) and (21 dB), the creators of [8] had to sacrifice a large antenna area. According to [26], the isolation is 17 dB when using the parasitic decoupling structure. An excellent strategy for improving isolation has been widely acknowledged: using defective ground structure [3], [20], [28], [29], [31], [34]. Reference [20] presents an analysis of a small multiple-input multiple-output antenna with a split ring resonator and a flawed ground structure.

2. Materials and Methods

This antenna has two ports and was designed for use in wideband environments. Although the antenna has a small footprint, it has a low gain, a relatively low efficiency, and a low isolation of 15 dB. Research in the field [3], [28], [29], [31] has shown that using a flawed ground of structure improves capabilities of isolation, but only up to a gain of less than 5 dBi. To attain a gain improvement of up to 9 dBi, the authors of the aforementioned study [34] used a size-diverse technique in combination with a flawed ground of structure. On the other hand, keep in mind that the whole construction dimensions of the antenna are 200×150 mm, which could be seen as somewhat big when applied to IoT applications.

The antenna shows very little isolation, even if it is very large. Antenna designs proposed in many studies have slots included into them to improve isolation of element

[21], [27], [32]. A shaped like plus slot is used as a stub in the ground in reference [21] to improve isolation of antenna by up to 20 dB and gain created from cst by up to 4.3 dBi. A resistance-loaded stub grounded to the ground achieves a 20 dB level of isolation in Ref. [27]. On the other hand, the antenna's dimensions are somewhat large. In order to attain 15 dB of isolation, the authors of the aforementioned research [32] present a four-element of MIMO arrangement that makes use of a rectangular stub on the ground plane. An innovative Ultra-Wideband (UWB) antenna design is presented in the aforementioned work [30]. An orthogonal orientation and a Compact Coplanar Waveguide (CPW) is the type of feeding mechanism are used in this design to accomplish self-decoupling. A level of isolation like 20 dB was achieved by the antenna. But keep in mind that the antenna is somewhat large, and that its gain and efficiency are pitiful. An orthogonal 4-port Octagonal Shaped MIMO Antenna for self-decoupling is created in an additional publication [37].

Although the antenna is not small, the authors have managed to obtain a 20 dB isolation. In [35], the authors talk about a slotted four-port MIMO antenna that looks like a spanner. Antenna isolation is just 10 dB because of its direction. Analyzed in a separate publication [38] is a small four-element multiple-input multiple-output antenna that is asymptote-shaped. Despite its small stature, the antenna boasts a robust isolation of 16 dB. Another well-known way to increase gain and isolation in recent years is meta-surfaces. In [22], [36], the writers increase segregation by up to 20 dB using metamaterials. In order to enhance gain and isolation, meta surface is utilized in [23], [24]. Despite being relatively large and having just 15.5 dB of isolation, the antenna manages a maximum gain of 8 dBi. Despite the antenna's low efficiency, the authors of [24] claim a 20 dB isolation.

3. Results and Discussion

This study proposes a slotted antenna in the shape of a grape leaf, fastened to the ground by a short stub. A pick realized gain of 8 dBi, an isolation of 25.5 dB, and a bandwidth of 1.9-20 GHz with a -10 dB drop are its features. The antenna is quite small in comparison to existing literature, and its maximum efficiency is close to 90%. Ideal for V2X communications, smart home, business, mall, and bus stop interior communications, the suggested antenna work for iot or wide band

Figure 1 shows a possible use case for the proposed antenna in an IoT environment, where users can exchange data with one another and with automobiles, as well as view traffic conditions. In addition, with the use of broadcast satellite communication and the internet, anyone can view any live broadcast. The car's location can be confirmed through communication with another vehicle. Soon, multi-system communication will be used for indoor communications in smart homes and retail areas. To allow communication between difference cars on the ITS-G5/802.11p band (5.9 GHz), the antenna can be installed in an intelligent system as shown in Figure 1. Various frequencies can be utilized by vehicles, including the 7.5 GHz satellite downlink band, the 2.4 GHz Bluetooth band, the 2.5 GHz and 5.5 GHz this two band as WLAN bands, the ISM bands (2.4 GHz and 5.8 GHz), and others [39], [40], [41]. In addition, the antenna is capable of covering the direct broadcast-satellite (DBS) band (17.3-18.4 GHz) [43] and the satellite uplink band (14.5-14.5 GHz) [42], [43]. To achieve a 4×4 MIMO arrangement, the antennas of each neighboring node are orthogonally translated, with a separation spacing of 8 mm. One uses an independent ground plane to deal with near-field coupling issues and to avoid surface currents [44]. Due to the near proximity of the antenna parts, a complex decoupling device or the removal of the ground plane is required.

Machine Learning (ML) prediction for efficiency and gain verification

Antenna designers have been heavily researching and using ML approaches for the last decade because of their capacity to learn from simulated antenna data through a training procedure [45], [46]. Manufacturing mistakes could cause the measured result to

be inaccurate. A large number of researchers have validated the antenna results using the ML prediction method. This research uses machine learning prediction to confirm the actual gain and efficiency of the proposed single-element antenna. Using a supervised regression ML approach, an accurate forecast of the antenna's actual parameter like gain and efficiency is produced.

Machine Learning(ML) implementation is two-step process. The first step is to collect pertinent information. Massive datasets are ideal for machine learning. The next step is to train machine learning models on the dataset and see which ones produce the best predictions. An ultra-wideband antenna is initially developed. The antenna's ground, feedline, slots, and stub are subsequently subjected to parametric sweeps [47]. The antenna results are greatly affected by these factors. Machine learning regression methods can sometimes benefit from bigger datasets. How much a bigger dataset affects a regression model depends on a lot of things, such as the problem's complexity, the number of input characteristics' dimensions, and the model's level of sophistication. Phase two entails using a range of regression machine learning (ML) techniques to estimate the proposed antenna's realized gain and efficiency, following the collection of 203 data samples through simulation using CST MWS. You can split the dataset into two pieces, one for testing and one for training. This approach uses statistical evidence to back up its random data split into training and testing sets. Predictions from four separate ML systems were used in this study. A variety of regression models are being considered, such as XGB, decision tree, random forest, and linear regression. We chose these algorithms because of how well they handle non-linear regression. Because of its emphasis on numerical output, regression is the ideal method for implementing predictions [48]. Flowchart representation of the steps involved in creating a dataset of machine learning and executing algorithm may be shown in Figure 1. I have prepared the dataset and divided it into two sections so that each may be studied independently. All machine learning studies were conducted in Google Colab, a Python simulation. To begin, split the dataset of machine learning in half lengthwise; put 80% into train and 20% into test, as suggested in [49]. Algorithms for machine learning will follow.

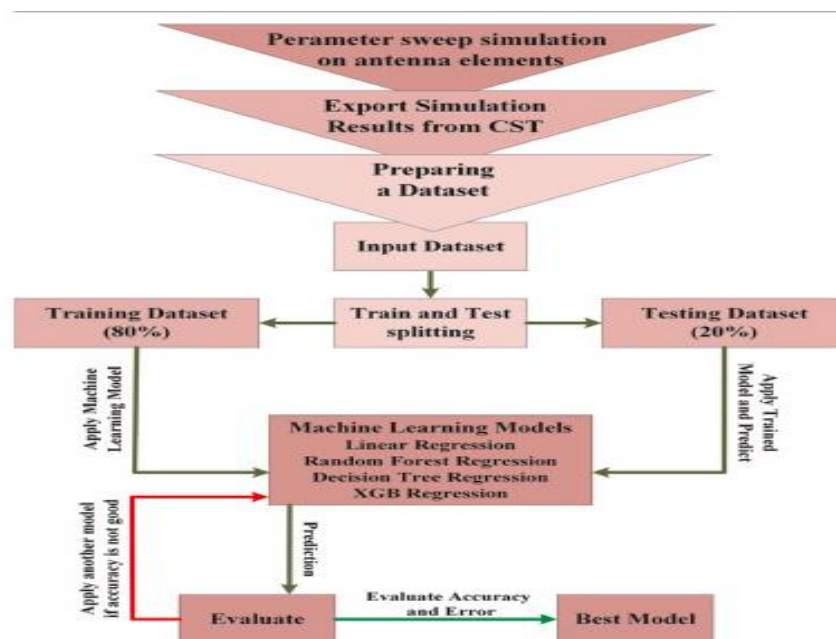


Figure 1. Flowchart ML process.

Evolution of proposed single element

In Figure 2, we can see the planned configuration of the single-element antenna. At its front, the antenna has a patch with ten triangle slots and two rectangular slots that are connected to a transmission line. Attached to the antenna's back side is a rectangular stub that is partially grounded. Careful engineering on the state-of-the-art Rogers-5880 substrate guarantees the antenna's peak performance and unwavering dependability. Figure 3 displays the individual component's temporal history, and Figure 4 shows the -10 dB frequency range it is the level of signal for each stage. It is clear that the -10 dB bandwidth starts at 2.6 GHz and goes up to 9.3 GHz, since there is no space on the patch. An arrangement with five perfectly cut slots on the right side of antenna in first part like the patch yields the appropriate frequency ranges of 2.7-9.7 GHz and 10.7-16 GHz. To achieve the desired result of several bands (3- GHzto 13.7 GHz, and 14.6-17 GHz), ten slots on either side of the patch can be implemented. Concurrently, a frequency band is efficiently attenuated by inserting two slots into the first part patch that is adjacent to the transmission of antenna line. Incorporating a ground-connected stub at the antenna's rear also helps achieve the desired from wide band characteristics, which extend from (2.1 to 19 GHz). A fundamental of difference rectangular patch with a partial ground plane and a resonant frequency of 3.5 GHz were the building blocks of the design. The transmission line model allows one to obtain a good approximation of the patch width of the antenna, as shown in Eq. (1).

$$Wp \approx \frac{c}{4f_{res} \sqrt{\frac{\epsilon_r + 1}{2}}}$$

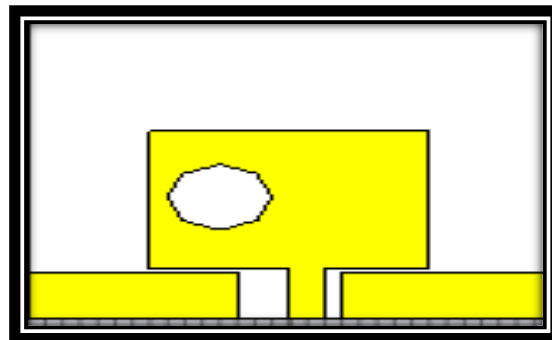


Figure 2. Front and Back View of single element.

The figure 3 illustrates a MIMO (Multiple-Input Multiple-Output) antenna element, characterized by its distinct geometric structure. The yellow regions represent conductive elements, while the white background indicates the substrate. The presence of slot-shaped apertures suggests enhanced radiation properties or impedance matching. The structured design indicates optimization for efficient signal transmission and reception in wireless communication systems.

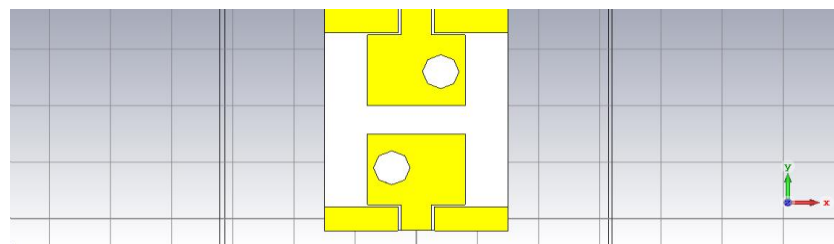


Figure 3. MIMO element.

The figure 4 presents the reflection coefficient (S_{11}) of a MIMO antenna across a frequency range of 1 to 8 GHz. The red and green curves represent different antenna elements, depicting resonance points where significant impedance matching occurs. The observed dips indicate optimal operational frequencies with minimized signal reflection, enhancing radiation efficiency.

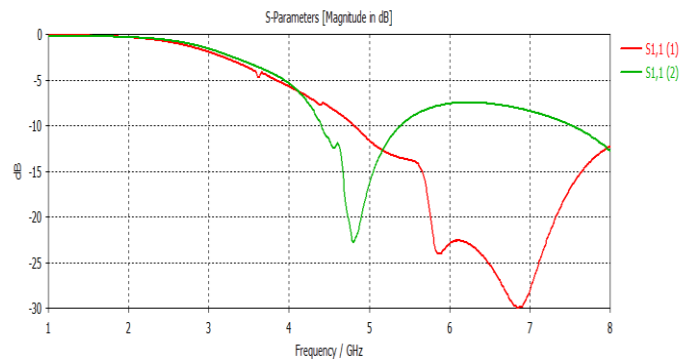


Figure 4. Reflection Coefficient.

The Table 1 presents the performance evolution from a single antenna element to a 4×4 MIMO configuration with a metasurface. The integration of metasurfaces enhances gain (8 dB), efficiency (89%), and isolation (25.5 dB), while maintaining a wide bandwidth (1.9–20 GHz). These improvements indicate optimized antenna performance for advanced wireless applications.

Table 1. Performance evolution single element to 4×4 with surface.

Antenna type	Single element	4×4 MIMO	4×4 MIMO with meta surface
Bandwidth	2.1–19	2–19	1.9–20
Gain	3.2	4.5	8
Efficiency	70	77	89
Isolation	—	20	25.5

Metrics For Measuring The Performance Of ML Models

The goal of linear regression [50] is to model the relationship between two variables by fitting a linear equation to the observed data. An explanation for the second variable—the more important one—is provided by the first variable.

An ensemble system, Random Forest [51] can handle regression and classification issues. The combination of the Bootstrap and Aggregation approach, often known as bagging, with several decision trees allows for this to be achieved.

Regression and classification models can also be built using decision trees. Decision tree regression [52] entails examining an item's properties and trains a model to fit into its tree structure. Afterwards, this model is employed to forecast upcoming data and consistently produce valuable outcomes.

A powerful implementation of the gradient-boosting technique, XGBoost [53] has numerous potential applications, including predictive regression modeling. When it comes to supervised regression analysis, XGBoost really comes into its own.

Among regression statistics, the error rate is by far the most used. Using a variety of statistical criteria, this study compared the performance of numerous ML algorithms. Difference type of Mean (MSE), (MAE), and (MSLE) were the error measures of choice for the ML process, while the variance score and coefficient of determination (R2) were used to quantify prediction accuracy. Mean squared error (MSE) shapes are common in regression loss functions. For each data point, we may calculate the loss by squaring the discrepancy between the expected and actual values. Equation (2) shows the formula for the MSE [54].

$$MSE = \frac{1}{n} \sum_{i=1}^n (y_i - \hat{y}_i)^2$$

As a general rule, the difference between expected and actual values can be found using mean absolute error (MAE). Equation (3)

$$MAE = \frac{1}{n} \sum_{i=1}^n |y_i - \hat{y}_i|$$

demonstrates the MAE [55] formulation. Here, n is the number of errors, and an is the absolute inaccuracy. As a comparison of actual and estimated values, the MSLE can be seen as a useful tool. The MSLE equation is shown in Eq. (4) [56].

$$MSLE = \frac{1}{n} \sum_{i=1}^n (\log(y_a) - \log(y_p))^2$$

The model's fit to the data is evaluated using the R-squared statistic. The closer R2 gets to 1, the better the model fits the data; the farther it gets from 0, the worse the model fits the data. A negative R-squared value may be produced if the model foretells a very unlikely outcome. Equation (5)

$$R^2 = 1 - \frac{\sum_{i=1}^N (y_i - \hat{y}_i)^2}{\sum_{i=1}^N (y_i - \bar{y})^2}$$

is the expression for the R-squared value [57]. The explained variance score [58] describes the error dispersion of each dataset. For the technical description, see Eq. (6).

$$\text{Explained variance } (y, \hat{y}) = 1 - \frac{\text{Var}(y - \hat{y})}{\text{Var}(y)}$$

Analyze verification gains

The regression methodologies that are analyzed and contrasted in Table 1 include linear regression, random forest, decision tree regressor, and XGB methods, among others. The accuracy of each technique is evaluated using a variety of metrics, such as variance score, R-squared, mean squared logarithmic error (MSLE), mean squared absolute error (MAE), and mean squared squared (MSE). On top of that, Fig. 2 shows a bar chart that compares the results of the models. Minimal MAE, MSE, and MSLE scores of 0.0038, 0.00003, and 0.000001, respectively, are shown for the Linear Regression or poly regression model. Also, with difference type of measure like R-squared and variance score precision of 98.7971% and 98.7972%, respectively, LR is the most accurate method available. The discrepancy between the predicted and predicted LR increases for a group of 41 test samples is negligible, if not nonexistent, as shown in Figure 3. Furthermore, there is a rate of error that is lower than 1% on average. A 93% or higher accuracy rate is reported by every one of the available Regression models. It is reasonable to assume that the antenna gain is almost exactly as expected (as shown in Fig. 3 as the simulation, given how closely they match.

The Table 2 presents the performance metrics of machine learning regressors for gain prediction. Linear Regression achieves the highest accuracy with an R2R^2R2 of 99.7971%, followed by XGB Regression (98.6283%). Decision Tree Regression exhibits the lowest

performance ($R^2 = 93.8762\%$). Lower MAE and MSE values indicate superior predictive capabilities.

Table 2. Performance metrics of ML regressors for gain.

Algorithms	MAE	MSE	MSLE	R^2	Var Score
Linear Regression	0.0038	0.00003	0.000001	99.7971%	99.7972%
XGB Regression	0.0091	0.00020	0.000008	98.6283%	98.6397%
Random Forest Regression	0.0125	0.00052	0.000020	96.6233%	96.6822%
Decision Tree Regression	0.0189	0.00095	0.000038	93.8762%	93.9339%

The bar chart compares the performance of machine learning regressors for gain prediction using R^2 and variance score metrics. Linear Regression outperforms others with nearly 100% accuracy, followed by XGB Regression. Random Forest and Decision Tree regressions show lower accuracy, indicating their relatively lower predictive efficiency for gain estimation in this context, see Figure 5.

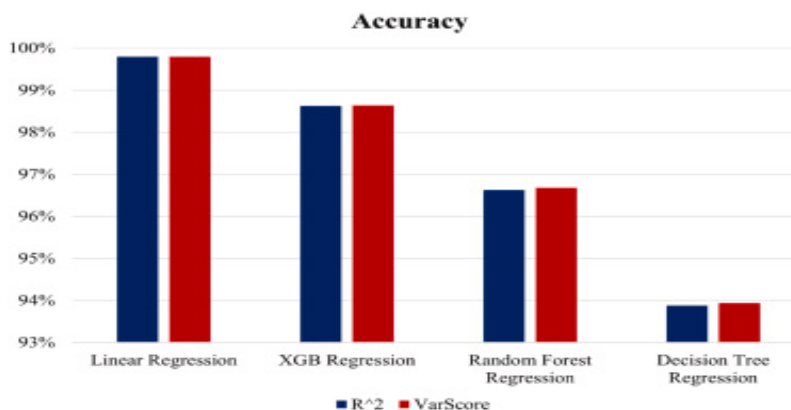


Figure 5. Performance comparative bar chart of ML regressors For Gain

The Table 3 presents performance metrics of machine learning regressors for efficiency prediction. Linear Regression achieves the highest accuracy with an R^2 of 99.8961%, followed by XGB Regression (98.4352%). Decision Tree Regression exhibits the lowest performance ($R^2 = 94.0802\%$). Lower MAE and MSE values indicate better predictive performance across the models.

Table 3. Performance metrics of ML regressors for Efficiency.

Algorithms	MAE	MSE	MSLE	R^2	Var Score
Linear Regression	0.0578	0.0150	0.000004	99.8961%	99.8992%
XGB Regression	0.2806	0.2261	0.000056	98.4352%	98.4418%
Random Forest Regression	0.3377	0.4100	0.000105	97.1633%	97.2629%
Decision Tree Regression	0.4348	0.8555	0.000215	94.0802%	94.3641%

Assessment of efficiency

Linear, random forest, decision tree regression, and XGB regression approaches are compared and contrasted in Table 3. Each algorithm is assessed for its accuracy using the following metrics: R-squared, variance score, mse, msles and absolute meaning of the error. On these three metrics, the LR model has demonstrated to generate small inaccuracies (0.05787, 0.0150, and 0.000004). With an MSE of 0.8555, Decision Tree outperformed all of methods we examined. In contrast, when compared to the MSLE benchmark, Decision Tree Regression has the tiniest inaccuracy. The LR has the best prediction accuracy for both the R-squared and variance scores, coming in at 99.8961% and 99.8992%, respectively. Figure 4 also includes a bar chart that compares and contrasts the models' performance. In Fig. 5, along with the predicted and predicted efficiency, we can see the outcomes of applying Gaussian Process Regression (GPR) to all 41 test samples. We customized the research frequency range to our desire, which falls between 2 and 20 GHz. The predicted and simulated efficiency values of the LR model are extremely similar, coming very near to zero, as seen in Figure 5. Hence, the predicted outcome is very similar to the representation of the simulated result. Even the other models have achieved accuracy rates higher than 94%. As a result, the LR method is the best bet for confirming efficiency, and the results from simulations are trustworthy.

The Figure 6 compares the performance of machine learning regressors for efficiency prediction using R^2 and variance score metrics. Linear Regression demonstrates the highest accuracy, followed by XGB Regression. Random Forest and Decision Tree regressions exhibit lower performance, indicating reduced predictive capabilities. The results highlight model suitability for efficiency estimation tasks.

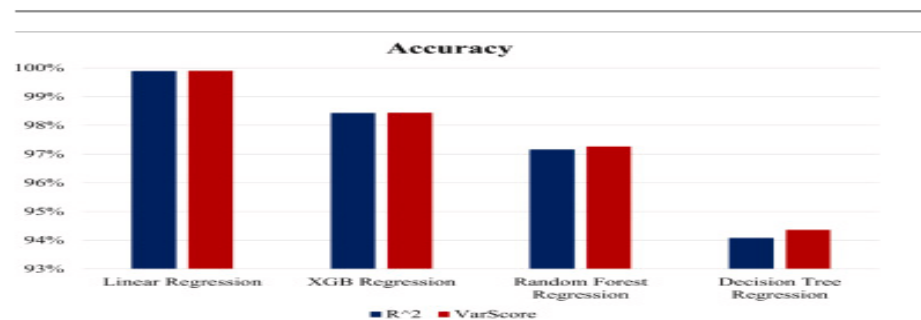


Figure 6. Performance of ml.

The figure 7 illustrates a comparison between simulated and predicted efficiency values across multiple observations. The blue solid line represents simulated data, while the red dashed line indicates predicted values. The close alignment between both curves suggests high model accuracy, demonstrating the effectiveness of the predictive approach in estimating efficiency trends.

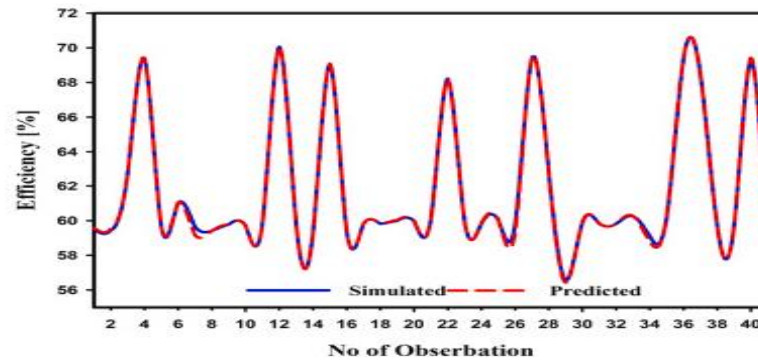


Figure 7. Simulated vs predicted.

4. Conclusion

Also, the full operational bandwidth RLC equivalent circuit is developed and confirmed to be consistent with CST simulation. Also, in order to make sure everything is correct, we use Machine Learning to forecast the single-element antenna's actual gain and efficiency. The exceptional performance of Linear regression—achieving an astounding 98% accuracy for both measure realized gain and efficiency verification—is highlighted among four algorithms regression models that are employed. Notably, the simulation results and prototype measurements are very congruent, which proves that our antenna design is correct. With its wide coverage across multiple IoT domains, the four-port MIMO antenna is clearly a good fit for 5G application and Internet of Things (IoT) applications, according to these results.

REFERENCES

- [1] R. K. Garg, S. Singhal, M. V. D. Nair, and R. Tomar, "A double-leaf-shaped four-port MIMO antenna for ultra-wideband applications," *Int. J. RF Microwave Comput.-Aided Eng.*, vol. 32, no. 11, Article e23349, 2022.
- [2] A. Khurshid, J. Dong, M. S. Ahmad, and R. Shi, "Optimized super-wideband MIMO antenna with high isolation for IoT applications," *Micromachines*, vol. 13, no. 4, p. 514, 2022.
- [3] R. Gomez-Villanueva and H. Jardon-Aguilar, "Compact UWB uniplanar four-port MIMO antenna array with rejecting band," *IEEE Antennas Wirel. Propag. Lett.*, vol. 18, no. 12, pp. 2543-2547, 2019.
- [4] A. Kumar, G. Saxena, P. Kumar, Y. K. Awasthi, P. Jain, S. S. Singhwal, P. Ranjan, "Quad-band circularly polarized super-wideband MIMO antenna for wireless applications," *Int. J. RF Microwave Comput.-Aided Eng.*, vol. 32, no. 6, Article e23129, 2022.
- [5] M. A. Jensen and J. W. Wallace, "A review of antennas and propagation for MIMO wireless communications," *IEEE Trans. Antennas Propag.*, vol. 52, no. 11, pp. 2810-2824, 2004.
- [6] M. A. Sufian, N. Hussain, A. Abbas, J. Lee, S. G. Park, and N. Kim, "Mutual coupling reduction of a circularly polarized MIMO antenna using parasitic elements and DGS for V2X communications," *IEEE Access*, vol. 10, pp. 56388-56400, 2022.
- [7] D. Potti, Y. Tusharika, M. G. N. Alsath, S. Kirubaveni, M. Kanagasabai, R. Sankararajan, S. Narendhiran, and P. B. Bhargav, "A novel optically transparent UWB antenna for automotive MIMO communications," *IEEE Trans. Antennas Propag.*, vol. 69, no. 7, pp. 3821-3828, 2021.
- [8] A. Abbas, N. Hussain, M. A. Sufian, J. Jung, S. M. Park, and N. Kim, "Isolation and gain improvement of a rectangular notch UWB-MIMO antenna," *Sensors*, vol. 22, no. 4, p. 1460, 2022.
- [9] M. A. Sufian, N. Hussain, H. Askari, S. G. Park, K. S. Shin, and N. Kim, "Isolation enhancement of a metasurface-based MIMO antenna using slots and shorting pins," *IEEE Access*, vol. 9, pp. 73533-73543, 2021.
- [10] M. Alibakhshikenari, B. S. Virdee, L. Azpilicueta, M. Naser-Moghadasi, M. O. Akinsolu, C. H. See, B. Liu, R. A. Abd-Alhameed, F. Falcone, I. Huynen, et al., "A comprehensive survey of metamaterial transmission-line based antennas: Design, challenges, and applications," *IEEE Access*, vol. 8, pp. 144778-144808, 2020.

- [11] M. Alibakhshikenari, E. M. Ali, M. Soruri, M. Dalarsson, M. Naser-Moghadasi, B. S. Virdee, C. Stefanovic, A. Pietrenko-Dabrowska, S. Koziel, S. Szczepanski, et al., "A comprehensive survey on antennas on-chip based on metamaterial, metasurface, and substrate integrated waveguide principles for millimeter-waves and terahertz integrated circuits and systems," *IEEE Access*, vol. 10, pp. 3668-3692, 2022.
- [12] M. Alibakhshi-Kenari, M. Movahhedi, and H. Naderian, "A new miniature ultra-wide band planar microstrip antenna based on the metamaterial transmission line," in *2012 IEEE Asia-Pacific Conference on Applied Electromagnetics, APACE, IEEE, 2012*, pp. 293-297.
- [13] M. Alibakhshikenari, B. S. Virdee, P. Shukla, Y. Wang, L. Azpilicueta, M. Naser-Moghadasi, C. H. See, I. Elfergani, C. Zebiri, R. A. Abd-Alhameed, et al., "Impedance bandwidth improvement of a planar antenna based on metamaterial-inspired T-matching network," *IEEE Access*, vol. 9, pp. 67916-67927, 2021.
- [14] M. Alibakhshikenari, F. Babaeian, B. S. Virdee, S. Aïssa, L. Azpilicueta, C. H. See, A. A. Althuwayb, I. Huynen, R. A. Abd-Alhameed, F. Falcone, et al., "A comprehensive survey on various decoupling mechanisms with focus on metamaterial and metasurface principles applicable to SAR and MIMO antenna systems," *IEEE Access*, vol. 8, pp. 192965-193004, 2020.
- [15] M. Alibakhshikenari, M. Khalily, B. S. Virdee, C. H. See, R. A. Abd-Alhameed, E. Limiti, "Isolation enhancement of densely packed array antennas with periodic MTM-photonic bandgap for SAR and MIMO systems," *IET Microw. Antennas Propag.*, vol. 14, no. 3, pp. 183-188, 2020.
- [16] M. Alibakhshikenari, M. Khalily, B. S. Virdee, C. H. See, R. A. Abd-Alhameed, E. Limiti, "Mutual coupling suppression between two closely placed microstrip patches using EM-bandgap metamaterial fractal loading," *IEEE Access*, vol. 7, pp. 23606-23614, 2019.
- [17] M. Alibakhshikenari, M. Khalily, B. S. Virdee, C. H. See, R. A. Abd-Alhameed, E. Limiti, "Mutual-coupling isolation using embedded metamaterial EM bandgap decoupling slab for densely packed array antennas," *IEEE Access*, vol. 7, pp. 51827-51840, 2019.
- [18] A. Iqbal, A. Altaf, M. Abdullah, M. Alibakhshikenari, E. Limiti, S. Kim, "Modified U-shaped resonator as decoupling structure in MIMO antenna," *Electronics*, vol. 9, no. 8, p. 1321, 2020.
- [19] M. Alibakhshikenari, B. S. Virdee, P. Shukla, C. H. See, R. A. Abd-Alhameed, M. Khalily, F. Falcone, E. Limiti, "Antenna mutual coupling suppression over wideband using embedded periphery slot for antenna arrays," *Electronics*, vol. 7, no. 9, p. 198, 2018.
- [20] K. Patchala, Y. R. Rao, and A. Prasad, "Triple band notch compact MIMO antenna with defected ground structure and split ring resonator for wideband applications," *Heliyon*, vol. 6, no. 1, 2020.
- [21] A. Altaf, A. Iqbal, A. Smida, J. Smida, A. A. Althuwayb, S. Kiani Hassan, M. Alibakhshikenari, F. Falcone, E. Limiti, "Isolation improvement in UWB-MIMO antenna system using slotted stub," *Electronics*, vol. 9, no. 10, p. 1582, 2020.
- [22] A. H. Jabire, A. Ghaffar, X. J. Li, A. Abdu, S. Saminu, M. Alibakhshikenari, F. Falcone, E. Limiti, "Metamaterial-based design of compact UWB/MIMO monopoles antenna with characteristic mode analysis," *Appl. Sci.*, vol. 11, no. 4, p. 1542, 2021.
- [23] M. M. Hasan, M. T. Islam, M. Samsuzzaman, M. H. Baharuddin, M. S. Soliman, A. Alzamil, I. I. Abu Sulayman, M. S. Islam, "Gain and isolation enhancement of a wideband MIMO antenna using metasurface for 5G sub-6 GHz communication systems," *Sci. Rep.*, vol. 12, no. 1, p. 9433, 2022.
- [24] G. Saxena, Y. Awasthi, P. Jain, "Design of metasurface absorber for low RCS and high isolation MIMO antenna for radio location & navigation," *AEU-Int. J. Electron. Commun.*, vol. 133, Article 153680, 2021.
- [25] A. Abbas, N. Hussain, M. A. Sufian, W. A. Awan, J. Jung, S. M. Lee, N. Kim, "Highly selective multiple-notched UWB-MIMO antenna with low correlation using an innovative parasitic decoupling structure," *Eng. Sci. Technol. Int. J.*, vol. 43, Article 101440, 2023.
- [26] A. H. Jabire, S. Sani, S. Saminu, M. J. Adamu, M. I. Hussein, "A crossed-polarized four port MIMO antenna for UWB communication," *Heliyon*, vol. 9, no. 1, 2023.
- [27] S. K. Gupta, R. Mark, K. Mandal, S. Das, "Four element UWB MIMO antenna with improved isolation using resistance loaded stub for S, C, and X band applications," *Progress Electromagn. Res. C*, vol. 131, pp. 73-87, 2023.
- [28] S. Sharma, M. Kumar, "Design and analysis of a 4-port MIMO microstrip patch antenna for 5G mid band applications," *Progress Electromagn. Res. C*, vol. 129, pp. 231-243, 2023.
- [29] G. Ramyasree, N. Suman, "Compact 4-port Vivaldi MIMO antenna for 5G wireless devices," *Progress Electromagn. Res. C*, vol. 131, pp. 13-24, 2023.

- [30] S. Ahmad, S. Khan, B. Manzoor, M. Soruri, M. Alibakhshikenari, M. Dalarsson, F. Falcone, "A compact CPW-fed ultra-wideband multi-input-multi-output (MIMO) antenna for wireless communication networks," *IEEE Access*, vol. 10, pp. 25278-25289, 2022.
- [31] L. Matta, B. Sharma, M. Sharma, "Design of a catenary shaped multiband-MIMO antenna for ultra-wideband applications," *2023 IEEE Devices for Integrated Circuit, DevIC*, IEEE, pp. 335-340, 2023.
- [32] S. K. Mahto, A. K. Singh, R. Sinha, M. Alibakhshikenari, S. Khan, and G. Pau, "High isolated four element MIMO antenna for ISM/LTE/5G (Sub-6GHz) applications," *IEEE Access*, 2023.
- [33] Z. Zhou, Y. Ge, J. Yuan, Z. Xu, and Z. D. Chen, "Wideband MIMO antennas with enhanced isolation using coupled CPW transmission lines," *IEEE Trans. Antennas Propag.*, vol. 71, no. 2, pp. 1414-1423, 2023.
- [34] S. Nandedkar and S. Nawale, "Frequency and space diverse MIMO antenna with enhanced gain," *J. Integr. Sci. Technol.*, vol. 11, no. 2, p. 482, 2023.
- [35] N. Salim, M. S. Singh, A. T. Abed, and M. T. Islam, "4X4 MIMO slot antenna spanner shaped low mutual coupling for Wi-Fi 6 and 5G communications," *Alex. Eng. J.*, vol. 78, pp. 141-148, 2023.
- [36] F. Urimubenshi, D. B. Konditi, J. de Dieu Iyakaremye, P. M. Mpele, and A. Munyaneza, "A novel approach for low mutual coupling and ultra-compact two port MIMO antenna development for UWB wireless application," *Heliyon*, vol. 8, no. 3, 2022.
- [37] M. A. Abdelghany, M. F. A. Sree, A. Desai, and A. A. Ibrahim, "4-port octagonal shaped MIMO antenna with low mutual coupling for UWB applications," *CMES-Comput. Model. Eng. Sci.*, vol. 136, no. 2, pp. 1999-2015, 2023.
- [38] A. Wu, Y. Tao, P. Zhang, Z. Zhang, and Z. Fang, "A compact high-isolation four-element MIMO antenna with asymptote-shaped structure," *Sensors*, vol. 23, no. 5, p. 2484, 2023.
- [39] T. Rani, S. C. Das, M. S. Hossen, L. C. Paul, and T. K. Roy, "Development of a broadband antenna for 5G sub-6 GHz cellular and IoT smart automation applications," *2022 12th International Conference on Electrical and Computer Engineering, ICECE*, IEEE, pp. 465-468, 2022.
- [40] B. Feng, J. Chen, S. Yin, Z. Zhao, et al., "A tri-polarized antenna with diverse radiation characteristics for 5G and V2X communications," *IEEE Trans. Veh. Technol.*, vol. 69, no. 9, pp. 10115-10126, 2020.
- [41] C. X. Mao, S. Gao, and Y. Wang, "Dual-band full-duplex Tx/Rx antennas for vehicular communications," *IEEE Trans. Veh. Technol.*, vol. 67, no. 5, pp. 4059-4070, 2018.
- [42] S. Manshari, S. Koziel, and L. Leifsson, "Compact dual-polarized corrugated horn antenna for satellite communications," *IEEE Trans. Antennas Propag.*, vol. 68, no. 7, pp. 5122-5129, 2020.
- [43] M. E. Carkaci and M. Secmen, "Design and prototype manufacturing of a feed system for Ku-band satellite communication by using 3D FDM/PLA printing and conductive paint technology," *Int. J. RF Microwave Comput.-Aided Eng.*, vol. 30, no. 4, Article e22062, 2020.
- [44] M. S. Khan, A. Iftikhar, R. M. Shubair, A.-D. Capobianco, B. D. Braaten, and D. E. Anagnostou, "Eight-element compact UWB-MIMO/diversity antenna with WLAN band rejection for 3G/4G/5G communications," *IEEE Open J. Antennas Propag.*, vol. 1, pp. 196-206, 2020.
- [45] M. A. Haque, D. Saha, S. S. Al-Bawri, L. C. Paul, M. A. Rahman, F. Alshanketi, A. Alhazmi, A. Rambe, M. Zakariya, and S. S. B. Hashwan, "Machine learning-based technique for resonance and directivity prediction of UMTS LTE band quasi Yagi antenna," *Heliyon*, vol. 9, no. 9, 2023.
- [46] M. A. Haque, M. Zakariya, S. S. Al-Bawri, Z. Yusoff, M. Islam, D. Saha, W. M. Abdulkawi, M. A. Rahman, L. C. Paul, and S. Sharker, "Quasi-Yagi antenna design for LTE applications and prediction of gain and directivity using machine learning approaches," *Alex. Eng. J.*, vol. 80, pp. 383-396, 2023.
- [47] M. A. Haque, M. Zakariya, N. S. S. Singh, M. A. Rahman, L. C. Paul, "Parametric study of a dual-band quasi-Yagi antenna for LTE application," *Bull. Electr. Eng. Inform.*, vol. 12, no. 3, pp. 1513-1522, 2023.
- [48] M. A. H. Talpur, S. H. Khahro, T. H. Ali, H. B. Waseem, and M. Napiyah, "Computing travel impedances using trip generation regression model: A phenomenon of travel decision-making process of rural households," *Environ. Dev. Sustain.*, vol. 25, no. 7, pp. 5973-5996, 2023.
- [49] Q. H. Nguyen, H.-B. Ly, L. S. Ho, N. Al-Ansari, H. V. Le, V. Q. Tran, I. Prakash, and B. T. Pham, "Influence of data splitting on performance of machine learning models in prediction of shear strength of soil," *Math. Probl. Eng.*, vol. 2021, pp. 1-15, 2021.
- [50] M. A. Haque, M. Rahman, S. S. Al-Bawri, Z. Yusoff, A. H. Sharker, W. M. Abdulkawi, D. Saha, L. C. Paul, M. Zakariya, "Machine learning-based technique for gain and resonance prediction of mid band 5G Yagi antenna," *Sci. Rep.*, vol. 13, no. 1, p. 12590, 2023.

-
- [51] D. Borup, B. J. Christensen, N. S. Mühlbach, and M. S. Nielsen, "Targeting predictors in random forest regression," *Int. J. Forecast.*, vol. 39, no. 2, pp. 841-868, 2023.
- [52] M. Rakhra, P. Soniya, D. Tanwar, P. Singh, D. Bordoloi, P. Agarwal, S. Takkar, K. Jairath, and N. Verma, "WITHDRAWN: Crop price prediction using random forest and decision tree regression: A review," 2021.
- [53] A. I. A. Osman, A. N. Ahmed, M. F. Chow, Y. F. Huang, and A. El-Shafie, "Extreme gradient boosting (Xgboost) model to predict the groundwater levels in Selangor Malaysia," *Ain Shams Eng. J.*, vol. 12, no. 2, pp. 1545-1556, 2021.
- [54] M. A. Haque, N. S. S. Sarker, N. Sawaran Singh, M. A. Rahman, M. N. Hasan, M. Islam, M. A. Zakariya, L. C. Paul, A. H. Sharker, G. E. M. Abro, et al., "Dual band antenna design and prediction of resonance frequency using machine learning approaches," *Appl. Sci.*, vol. 12, no. 20, p. 10505, 2022.
- [55] K. Harishkumar, Y. K. Yogesh, I. Gad, et al., "Forecasting air pollution particulate matter (PM2.5) using machine learning regression models," *Procedia Comput. Sci.*, vol. 171, pp. 2057-2066, 2020.
- [56] O. Istaiteh, T. Owais, N. Al-Madi, and S. Abu-Soud, "Machine learning approaches for covid-19 forecasting," *2020 International Conference on Intelligent Data Science Technologies and Applications, IDSTA, IEEE*, pp. 50-57, 2020.
- [57] A. Gelman, B. Goodrich, J. Gabry, and A. Vehtari, "R-squared for Bayesian regression models," *Amer. Statist.*, 2019.
- [58] J. M. Weiming, *Mastering Python for Finance*, Packt Publishing Ltd, 2015.